

# Statistics of WMAP ILC Map Temperature Fluctuations Towards Distant Radio Galaxies

O.V. Verkhodanov<sup>a</sup>, M.L. Khabibullina<sup>a</sup>

<sup>a</sup>Special Astrophysical Observatory of the Russian AS, Nizhnij Arkhyz 369167, Russia

Received September 6, 2010; accepted February 1, 2011.

For 2442 galaxies of the catalog, compiled based on the NED, SDSS, and CATS survey data with redshifts  $z > 0.3$  we conducted an analysis of the amplitude of temperature fluctuations in the cosmic microwave background (CMB) in the points, corresponding to the direction to these objects. To this end, we used the ILC map from the WMAP mission seven-year data release. We have estimated the dipole component of the background and tested the hypothesis of Kashlinsky on the existence of a “dark bulk flow”, determined for the estimated dipole component of the CMB WMAP by the value of the CMB anisotropy in the direction to the clusters of galaxies. We show that the amplitude of this dipole  $T_{max} = 0.012$  mK is located within the  $\sigma$  interval, estimated by Monte Carlo simulations for the Gaussian fluctuations of the CMB signal in the  $\Lambda$ CDM model. The low amplitude of the dipole indicates that it is impossible to confirm this hypothesis from the WMAP data. In addition, we studied the statistics of the fluctuation amplitude of the microwave signal in the direction to radio galaxies. A weakening of the absolute value of the mean signal in the corresponding fields was discovered.

**Key words:** Radio lines: galaxies—techniques: radar astronomy

## 1. INTRODUCTION

The studies of properties of the large-scale structure, reflected in the statistics of the Cosmic Microwave Background (CMB), are of particular interest in connection with the advent of new high-accuracy observations in the millimeter and submillimeter ranges [1, 2, 3, 4]. Using the data on galaxy clusters and the magnitude of the CMB signal fluctuations in the direction to their centers, where the signal fluctuations are caused by the Sunyaev-Zel’dovich effect (SZ) [5], we can estimate the cosmological parameters (the Hubble constant  $H_0$ , and the density parameter  $\Omega_0$ ) [6]. In addition, one of the components of the SZ effect—the kinematic SZ effect, caused by the proper motion of the cluster as a whole with respect to the CMB reference system—opens the possibility of studying the large-scale fluxes of matter. In particular, [7, 8] describe the study of large-scale “dark bulk flows” in motion of clusters of galaxies, based on the WMAP5 data and the catalog, compiled from the X-ray data and containing more than 1000 clusters. The authors have calculated the dipole from the CMB pixel values. The dipole is determined, in their opinion, by the kinematic SZ effect; it reveals a constant velocity, at least on the scale of 800 Mpc.

Note that despite the low WMAP sensitivity to the SZ effect due to the relatively poor resolution of the final map of the isolated CMB signal (the limiting spherical harmonics—a multipole—in the first WMAP releases for the ILC CMB map there is  $\ell_{max} \sim 100$ , or, in terms of resolution,  $\theta \sim 55'$  and in the seven-year release it is  $\ell_{max} \sim 150$  ( $\theta \sim 35'$ ), while the SZ effect for most of galaxy clusters is strongly manifested on the small scale:  $\theta < 10'$ ), the discussed effect is of great interest in terms of its manifestation in the ongoing Planck mission<sup>1</sup>.

Also note that despite the limitations on resolution (channel W has a better resolution of  $12.6'$  with the frequency of 94 GHz) and on the sensitivity of WMAP maps, various attempts to measure the SZ effect statistically have been made both in the population averaging (“stacking”) (see, e.g., recent papers [9, 10]), and directly for individual bright clusters, such as Coma [10], where the effect was observed. Diego and Partridge [9] used three channels: Q (43 GHz, FWHM =  $0.51^\circ$ ), V (61 GHz,  $0.35^\circ$ ) and W (94 GHz,  $0.22^\circ$ ) and obtained averaged profiles in the direction to known clusters. In

<sup>1</sup> <http://www.rssd.esa.int/Planck/>

particular, besides the presence of the desired signal and the growth of its amplitude with frequency, the authors found that the signal's value is lower than expected from the X-ray data, the fact that they linked with the presence of a point source in the cluster. The WMAP team [10] has conducted a similar study, using two channels: V and W. They also applied the averaging of different regions in the direction to known clusters with X-ray emission and evidenced the effect. In addition, they discovered that the effect can be traced down to the scales of  $\theta = 1.05^\circ$ . The signal on the scale of  $\theta = 0.58^\circ$  is considered as true, and that on the scale of  $\theta = 1.05^\circ$ —as a statistical fluctuation. At that, the authors [10] have concluded that the apparent effect for the averaged sources is consistent with that, expected from the X-ray observations. Let us emphasize that the evaluations are made for the source, producing the SZ effect, and averaged over the sky. Recent experiments, such as the one conducted on the Atacama Cosmology Telescope (ACT) [11] and Planck mission [12] already allow to isolate and see this effect directly.

Despite the fact that for most clusters the SZ effect is not directly visible in the WMAP data, it is estimated statistically. We believe that the approach proposed in [7, 8] deserves special attention. We develop it in this paper, using the amplitude of temperature fluctuations in the points, corresponding to the direction to distant radio galaxies from our survey for the analysis. To detect the possible “dark bulk flow” we need to evaluate the signal towards distant radio galaxies. A useful moment is the fact that the CMB signal in the ILC map of fluctuations is isolated using the channels, in which the SZ effect, if existing, will have a negative signal. Fortunately, the angular scale of the SZ effect, discovered by the WMAP team [10] corresponds to the resolution of the ILC map of seven-year observations.

In the standard scheme of galaxy formation, the radio source lights up as a result of a merger of galaxies, and formation of an accretion disk and jets, observed at radio and other wavelengths. As a rule (see reviews in [13, 14]), the most powerful radio galaxies, visible at large redshifts are identified with giant elliptical galaxies, which are mainly the central galaxies of clusters and are formed by merging. This property (radio emission) can be used to find distant clusters and protoclusters of galaxies. For example, [15] presents the results of a program, conducted with the ESO VLT telescope, searching for the emerging clusters of galaxies near the powerful radio galaxies at redshifts  $2 < z < 5.2$  with the radio fluxes  $B_{2.7\text{GHz}} > 10^{33} \text{ erg s}^{-1} \text{ Hz}^{-1} \text{ sr}^{-1}$ . The authors have selected 150 objects and examined the fields around nine of them. In the fields the authors

have selected the galaxies, emitting in Ly $\alpha$  (the so-called Ly $\alpha$ -emitters), the redshifts of which were measured. Using the data on spatial density of objects it was concluded whether they belong to protoclusters. The size of such protoclusters is at least 1.75 Mpc. It was shown that 75% of radio galaxies with  $z > 2$  are associated with protoclusters. Hence, we can estimate that approximately  $3 \times 10^{-8}$  of the forming clusters lay in the interval of  $2 < z < 5.2$  in the comoving unit volume with a side of 1 Mpc with an active radio source. But it is likely that within a given range of redshifts the number of protoclusters may be higher, since an active radio source may simply not be observed.

Using the survey of remote (for example,  $z > 0.3$ ) radio galaxies, we can track the locations of clusters and protoclusters of galaxies, which in turn may affect the fluctuations of the microwave background. A sample of radio galaxies, prepared by us earlier [16, 17, 18] is very suitable to this end, and we use it in our study.

## 2. DATA ANALYSIS

### 2.1. Input Arrays

A sample of radio galaxies with  $z > 0.3$  [16, 17, 18, 19, 20] was constructed using the tools and archives of the following databases: NED<sup>2</sup>, CATS<sup>3</sup> [21, 22], SDSS<sup>4</sup> [23] with the aim to use it in various statistical and cosmological tests [13, 24, 25], which require an analysis of a large sample of objects of the same nature. The NED database was used to construct the primary list of objects. We selected from it the objects with required parameters, mainly based on redshift ( $z > 0.3$ ) and morphological properties of radio galaxies. The initial catalog contained 3364 objects. Such a sample of galaxies is contaminated with objects with incomplete information, or objects with other properties. Therefore, special attention was paid to clean the original sample from the odd sources: galaxies (1) with redshifts, determined by the photometric method; (2) those with quasar properties from the available literature data. The final catalog contains 2442 sources with spectroscopic redshifts, the photometric values and flux densities in the radio range, the sizes of radio sources, as well as radio spectral indices, which were calculated based on the results of cross-identification with the radio catalogs, stored in the CATS, in the frequency range

<sup>2</sup> <http://nedwww.ipac.caltech.edu>

<sup>3</sup> <http://cats.sao.ru>

<sup>4</sup> <http://www.sdss.org>

from 325 MHz to 30 GHz. The positions of 2442 galaxies on the sphere are demonstrated in Fig. 1.

As the CMB map, we used the map of the distribution of the cosmic microwave background anisotropy, reconstructed based on the multi-frequency observations via the technique of internal linear combination (ILC) of the background components [1] in the observational program of the WMAP space mission<sup>5</sup> (Wilkinson Microwave Anisotropy Probe). To construct the WMAP map, the data in five bands were used: 23 GHz (K-band), 33 GHz (Ka-band), 41 GHz (Q-band), 61 GHz (V-band), and 94 GHz (W-band). The ILC map contains information on the distribution of the microwave background for not very high harmonics ( $\ell \leq 150$ ).

Nevertheless, it is currently the most tested and used CMB map. For the data analysis, we use the distribution of the signal  $\Delta T(\theta, \phi)$ , describing the temperature anisotropy on the sphere, with two limiting values (by angular resolution) of the multipoles  $\ell_{max} \leq 150$  ( $\theta \geq 36'$ ) and  $\ell_{max} \leq 20$  ( $\theta \geq 260'$ ) according to the decomposition into spherical harmonics:

$$\Delta T(\theta, \phi) = \sum_{\ell=2}^{\infty} \sum_{m=-\ell}^{m=\ell} a_{\ell m} Y_{\ell m}(\theta, \phi),$$

where the spherical harmonics is

$$Y_{\ell m}(\theta, \phi) = \sqrt{\frac{(2\ell+1)(\ell-m)!}{4\pi(\ell+m)!}} P_{\ell}^m(x) e^{im\phi},$$

$x = \cos\theta$   $P_{\ell}^m(x)$  are the associated Legendre polynomials,  $\ell$  and  $m$  are the multipole number and its modes, respectively. For the expansion of spherical harmonics, we used the GLESP package<sup>6</sup> [26].

## 2.2. Signal Histograms in CMB Pixels

To analyze the Gaussianity of the distribution in the first order and compare it with the model, we took the amplitude of CMB signal fluctuations in the map pixels, onto which the radio galaxies are projected (Fig. 2), and constructed the histograms of its distribution (Fig. 3). One of the rules of galaxy selection in our sample was the presence of a spectroscopic redshift, measured, as a rule, in objects outside the Galactic plane, hence the lack of sources in the central band of Fig. 2 (the Galactic plane) is a selection effect. The pixel size of maps, used for the analysis, at resolutions of  $\ell_{max} \leq 150$  and  $\ell_{max} \leq 20$  amounts to  $36' \times 36'$  and  $260' \times 260'$ , respectively. The analysis

was carried out for maps with  $\ell_{max} \leq 150$ , since the ILC data in the WMAP7 release are presented with a better resolution.

Figure 3 shows the corresponding histograms for the CMB fluctuation amplitude distributions of the ILC map in pixels, corresponding to the direction to the catalog radio galaxies. The histograms present a  $1\sigma$ -spread, calculated by two methods on the pixel statistics: (1) for the given 100 realizations of the microwave background maps in the  $\Lambda$ CDM cosmological model with homogeneous and isotropic Gaussian random fields, resulting in the corresponding CMB fluctuations, and (2) for 100 realizations of a random arrangement of 2442 points in the ILC WMAP7 map itself. The value of the histogram bean is 0.02 mK.

Note the particularities of the distributions shown in Fig. 3. All the signal variation distributions in the studied pixels are close to normal. The distribution maximum  $N$  is located strictly in the region of zero amplitude fluctuations. Its value exceeds the mean expected level by more than  $3\sigma$  for the maps with a resolution of  $\ell_{max} \leq 150$  and about  $2\sigma$  with  $\ell_{max} \leq 20$  for the spread estimates, calculated using the Monte Carlo method for Gaussian background fluctuations in the  $\Lambda$ CDM cosmology (left graphs of the figure), and over  $2\sigma$  for the estimates, obtained in randomly selected pixels of the ILC map. The estimates are presented in the Table.

In addition, for both resolutions  $\ell = 150$ , and  $\ell = 20$ , the ratio  $(T_{max}/T_{min})^{ledm} > (T_{max}/T_{min})^{ile}$ , indicating a lower dispersion of signal variations in the map than that, expected in the  $\Lambda$ CDM model.

## 2.3. Dipole Estimation

Using the value of temperature fluctuations in pixels in the map with a resolution of  $\ell = 150$ , applying the least-squares method we estimated the corresponding dipole in the form

$$T(l, b) = T_x \cos(l) \cos(b) + T_y \sin(l) \cos(b) + T_z \sin(b),$$

where  $(l, b)$  are the galactic coordinates: longitude and latitude,  $T(l, b)$  is the value of CMB temperature fluctuations in mJy, taken in the pixels corresponding to the positions of radio galaxies, and  $(T_x, T_y, T_z)$  are the dipole components, which are found to be equal to (0.0116, 0.0036, 0.0026), respectively.

Hence, we obtain the following for the extrema:

$$T_{extrem} = \pm \sqrt{T_x^2 + T_y^2 + T_z^2},$$

$$b = \pm \arctan(T_z / \sqrt{T_x^2 + T_y^2}),$$

$$l = \arctan(T_y / T_x),$$

<sup>5</sup> <http://lambda.gsfc.nasa.gov>

<sup>6</sup> <http://www.glesp.nbi.dk>

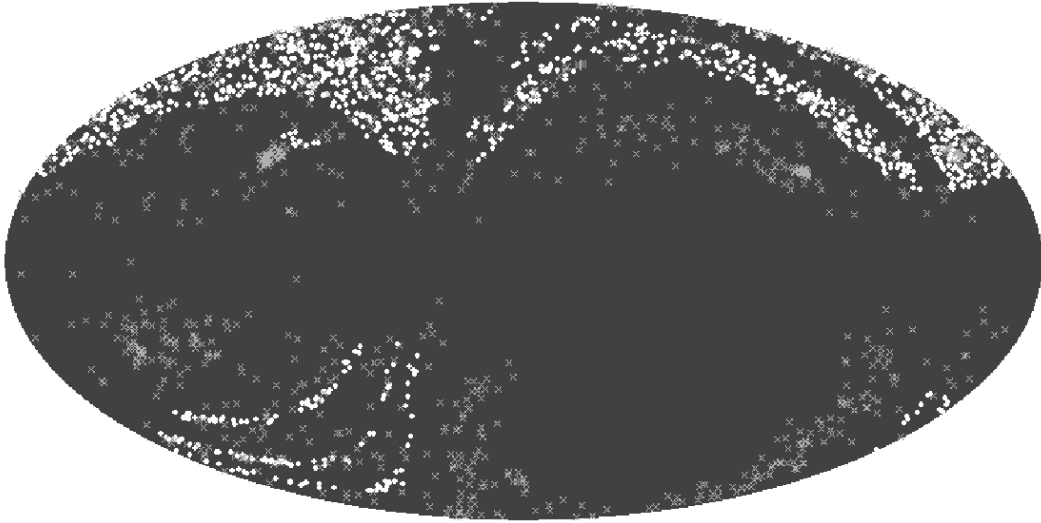


Figure 1: Position of selected radio sources on the celestial sphere in galactic coordinates. White circles mark the SDSS objects, gray crosses—the remaining sources.

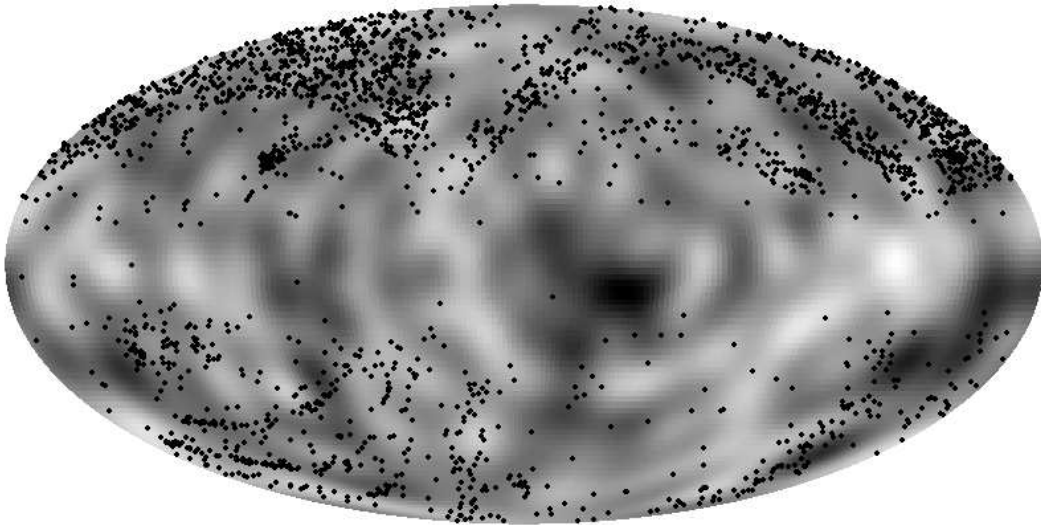


Figure 2: Position of selected galaxies (black circles) in the CMB WMAP map with a resolution of  $\ell_{max} = 20$  in galactic coordinates. Dark spots in the map correspond to the cold signal, while light spots—to the hot signal.

or in the maximum  $T_{max} = 0.0124$  mK with coordinates  $(l_{max}, b_{max}) = (17^\circ.307, 11^\circ.844)$ , and in the minimum  $T_{min} = -0.0124$  mK with coordinates  $(l_{min}, b_{min}) = (197^\circ.307, -11^\circ.844)$ . The dipole's position on the sphere is shown in Fig. 4.

Despite the fact that the estimated dipole is visually “drawn” towards the Galactic center, the significance of its position, as well as the reality of its existence seems doubtful in view of its small amplitude:  $T_{max} = 0.012$  mK. This value lays within the  $\sigma$ -scatter from the mean, i.e. within the noise, estimated by modelling of 50 CMB signal realizations in the  $\Lambda$ CDM model, and determining the parameters of the

dipole in each of the realizations for the coordinates of the radio galaxy catalog. The modelling results yield an average estimate of the parameters  $(T_x, T_y, T_z) = (0.003 \pm 0.016, 0.001 \pm 0.018, -0.002 \pm 0.010)$ .

### 3. RESULTS

We investigated the properties of the CMB WMAP7 signal in the fields of distant ( $z > 0.3$ ) radio galaxies. In general, the signal distribution over the areas corresponds to normal. Moreover, in this distribution the histogram amplitude is higher than expected (more than by a  $\sigma$ -scatter) both for the  $\Lambda$ CDM

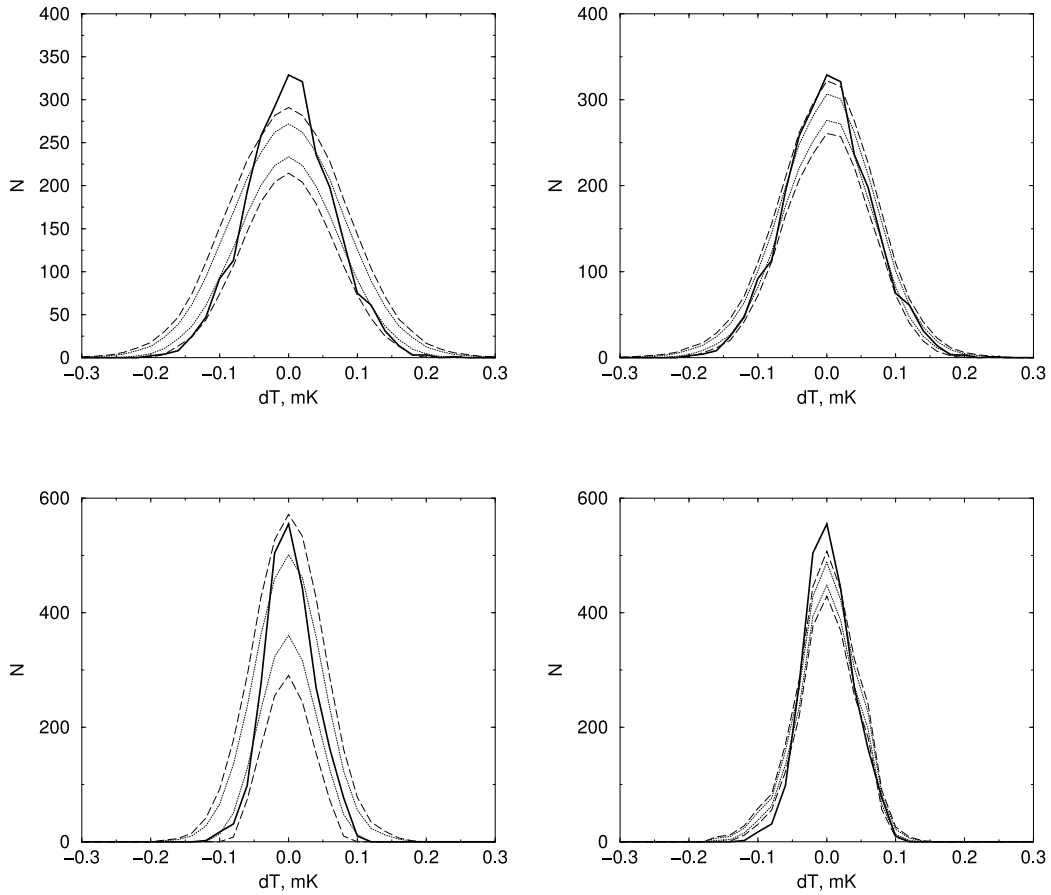


Figure 3: The histograms of the distribution of the microwave background signal value (the thick solid line) in the ILC map, measured in pixels, corresponding to the direction to radio galaxies. Above: histograms for the pixel map resolution of  $\ell_{max} \leq 150$ . Bottom: histograms for the pixel map resolution of  $\ell_{max} \leq 20$ . Left: the dotted and dashed lines show the levels of  $1\sigma$  and  $2\sigma$ -spreads, respectively, calculated from the data of 100 realizations of the  $\Lambda$ CDM cosmological model. Right: The dotted and dashed lines show the levels of  $1\sigma$  and  $2\sigma$ -spreads, respectively, calculated from the data of 100 realizations of a random distribution of points in the ILC WMAP seven-year map.

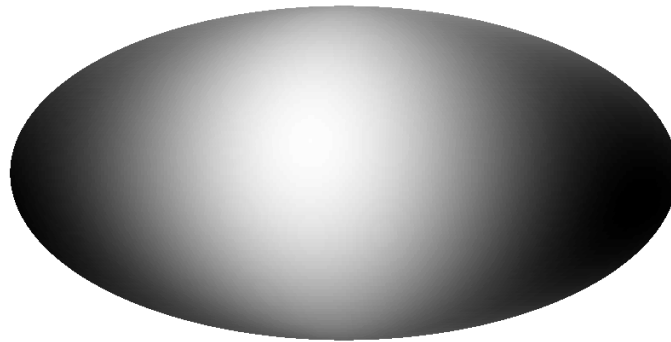


Figure 4: The position of the dipole on the sphere, determined with the least-squares method from the CMB pixel values in the locations of distant radio galaxies, in galactic coordinates.

Table 1: **Table.** Parameters of normal distribution (the amplitude  $N$  and the width parameter  $s_0 = \theta_{0.5}(8 \ln 2)^{-1/2}$ ), corresponding to the distribution of the CMB temperature fluctuation amplitude in the pixels of galaxy positions for maps with resolutions  $\ell = 150$  and  $\ell = 20$ . The estimates of the distribution of temperature minima and maxima at the  $\sigma$ -scatter are obtained when modeling the background fluctuations in 100 realizations of a random signal in the  $\Lambda$ CDM cosmological model (marked as *lcdm*), and in the simulations of 100 realizations of a random scatter of galaxy locations in the ILC map (noted as *ilc*).

Value Distribution	Amplitude $N$	$s_0$ , mK
$T(\ell = 150)$	319.2	0.060
$T_{min}(\ell = 150)^{lcdm}$	232.7	0.072
$T_{max}(\ell = 150)^{lcdm}$	271.0	0.082
$T_{min}(\ell = 150)^{ilc}$	276.1	0.064
$T_{max}(\ell = 150)^{ilc}$	304.4	0.068
$T(\ell = 20)$	552.6	0.035
$T_{min}(\ell = 20)^{lcdm}$	362.4	0.041
$T_{max}(\ell = 20)^{lcdm}$	501.1	0.049
$T_{min}(\ell = 20)^{ilc}$	438.8	0.041
$T_{max}(\ell = 20)^{ilc}$	474.5	0.043

cosmological model and for the random positioning of objects on the ILC WMAP map. That is, the pixels, corresponding to the direction to distant radio galaxies, are dominated by small (approaching zero) fluctuation values, which leads to an increase in the histogram amplitude above the expected value. Absence of a shift in the position of the histogram peak indicates either the absence of any signal in these pixels, or a compensation of the SZ effect by the radio emission of the galaxy (see, e.g., [9]). Theoretically, one could expect a shift either towards the negative signal in the case of the SZ effect, or towards the positive signal in the case of existence of a residuary signal from the radio source after the component separation. In the presence of both factors we would see an increase in the width of the histogram, compared with the simple models of the background perturbation. However, an inverse effect is observed: the resulting CMB WMAP7 signal distribution, measured in the regions of radio galaxy positions on the sphere is in fact narrower than the one, expected for random Gaussian fluctuations, and than the one, observed in the ILC map on the average. In addition, the variance of the  $s_0$  distribution is smaller than expected in models, which also indicates an increased number of pixels with zero signal in the fields of radio galaxies. And if the correlation  $(T_{max}/T_{min})^{lcdm} > (T_{max}/T_{min})^{ilc}$

can be explained by an underestimated value of the amplitude of the ILC quadrupole, then the cause of the effect of signal attenuation in the fields of radio galaxies is as yet unclear.

We as well tried to test the effect of existence of a dipole in the CMB data in the regions of galaxy clusters, discovered in [7, 8]. It is determined, as the authors suppose, by the kinematic SZ effect, and associated with the “dark bulk flow” of matter. To verify this phenomenon, we constructed a dipole using the values in the pixels of galaxy positions, and found that this dipole’s amplitude is below the  $\sigma$  noise level of model variations.

Note that the size of the ILC map pixel in general does not allow to valuably investigate the SZ effect. In addition, it is clear that the nonzero dipole can almost always be defined for a finite sample of pixels with nonzero values, what the models are demonstrating. Although we do not rule out the possibility that for the nearby clusters of galaxies the background fluctuations can show the existence of a common movement, distinct from the known CMB kinematic dipole, but for distant objects, as in our case, the Hubble flow will be dominating. We shall be able to check this effect after the publication of maps of the Planck mission.

## 4. ACKNOWLEDGMENTS

The authors are grateful to P. D. Naselsky for helpful discussions, to S. A. Trushkin for valuable comments that allowed to improve the text and to O. Nasonova for her aid with the calculations in the MATLAB package. In the study we used the NED database of extragalactic objects The authors also used the CATS [27] database of radio astronomy catalogs, the FADPS<sup>7</sup> [28, 29] system for processing the radio astronomy data, and the GLESP package data analysis of microwave radiation on the sphere [30, 31]. This work was supported by the Leading Scientific Schools of Russia (S. M. Khaikin school) grant, and the RFBR grants (project nos. 09-02-00298, 08-02-00486). O.V.V. is also grateful for the partial support of the Dmitry Zimin Dynasty Foundation.

## References

- C. L. Bennett, M. Halpern, G. Hinshaw, et al., *Astrophys. J. Supp.* **148**, 1 (2003), astro-ph/0302207.
- G. Hinshaw, D. N. Spergel, L. Verde, et al., *Astrophys. J. Supp.* **170**, 288 (2007), astro-ph/0603451.
- G. Hinshaw, J. L. Weiland, R. S. Hill, et al., *Astrophys. J. Supp.* **180**, 225 (2009), astro-ph/0803.0732.
- N. Jarosik, C. L. Bennett, J. Dunkley, et al., *Astrophys. J. Supp.*, submitted (2010), arXiv:1001.4744.
- Ya. B. Zeldovich and R. A. Sunyaev, *Astrophys. Space Sci.* **4**, 301 (1969).

<sup>7</sup> [http://sed.sao.ru/~vo/fadps\\_e.html](http://sed.sao.ru/~vo/fadps_e.html)

- G. De Zotti, R. Ricci, D. Mesa, et al., *A&A* **431**, 893 (2005), astro-ph/0410709.
- A. Kashlinsky, F. Atrio-Barandela, H. Ebeling, et al., *Astrophys. J* **712**, 81 (2010), astro-ph/0910.4958.
- F. Atrio-Barandela, A. Kashlinsky, H. Ebeling, et al., *Astrophys. J* **719**, 77 (2010), astro-ph/1001.1261.
- J. M. Diego and B. Partridge, *MNRAS* **402**, 1179 (2010).
- E. Komatsu, K. M. Smith, J. Dunkley, et al., *Astrophys. J. Supp.* **192**, 18 (2011), astro-ph/1001.4538.
- A. D. Hincks, V. Acquaviva, P. A. R. Ade, et al. *Astrophys. J. Supp.* **191**, 423 (2010).
- N. Aghanim, M. Arnaud, M. Ashdown, et al. (Planck Collaboration), *A&A*, submitted (2011), astro-ph/1101.2043.
- O. V. Verkhodanov and Yu. N. Parijskij, *Radiogalaktiki i kosmologija (Radio Galaxies and Cosmology)*, (Fiz. Math. Lit., Moscow, 2009) [in Russian].
- G. Miley and C. De Breuck, *Astron. Astroph. Rev***15**, 67 (2008).
- B. P. Venemans, H. J. A. Röttgering, G. K. Miley, et al., *A&A* **461**, 823 (2007).
- M. L. Khabibullina and O. V. Verkhodanov, *Astrophys. Bull.* **64**, 123 (2009), astro-ph/0911.3741.
- M. L. Khabibullina and O. V. Verkhodanov, *Astrophys. Bull.* **64**, 276 (2009), astro-ph/0911.3747.
- M. L. Khabibullina and O. V. Verkhodanov, *Astrophys. J. Suppl.* **64**, 340 (2009), astro-ph/0911.3752.
- O. V. Verkhodanov and M. L. Khabibullina, *Pis'ma Astron. Zh.* **36**, 9 (2010), astro-ph/1003.0577.
- M. L. Khabibullina and O. V. Verkhodanov, *Astron. Zh.* **88**, 333 (2011).
- O. V. Verkhodanov, S. A. Trushkin, H. Andernach and V. N. Chernenkov, *ASP Conf. Ser.* **125**, 322 (1997), astro-ph/9610262.
- O. V. Verkhodanov, S. A. Trushkin, H. Andernach and V. N. Chernenkov, *Bull. Spec. Astrophys. Obs.* **58**, 118 (2005), astro-ph/0705.2959.
- D. P. Schneider, P. B. Hall, G. T. Richards, et al., *AJ* **134**, 102 (2007).
- O. V. Verkhodanov and Yu. N. Parijskij, *Bull. Spec. Astrophys. Obs.* **55**, 66 (2003).
- O. V. Verkhodanov and Yu. N. Parijskij, in *Proc. 14th Internat. School Particles and Cosmology*, Ed. by S. V. Demidov, V. A. Matveev, and V. A. Rubakov (INR, Moscow, 2008), p. 109.
- A. G. Doroshkevich, P. D. Naselsky, O. V. Verkhodanov, et al., *Int. J. Mod. Phys. D* **14**, 275 (2003), astro-ph/0305537.
- O. V. Verkhodanov, S. A. Trushkin, H. Andernach and V. N. Chernenkov, *Data Science Journal* **8**, 34 (2009), astro-ph/0901.3118.
- O. V. Verkhodanov, *ASP Conf. Ser.* **125**, 46 (1997).
- O. V. Verkhodanov, B. L. Erukhimov, M. L. Monosov, et al., *Bull. Spec. Astrophys. Obs.* **36**, 132 (1993).
- O. V. Verkhodanov, A. G. Doroshkevich, P. D. Naselsky, et al., *Bull. Spec. Astrophys. Obs.* **58**, 40 (2005).
- A. G. Doroshkevich, O. B. Verkhodanov, P. D. Naselsky, et al., *Intern. J. Mod. Phys. D*, accepted (2011), astro-ph/0904.2517.